Molecular Therapy
Original Article

mRNA Delivery for Therapeutic Anti-HER2 Antibody Expression *In Vivo*

Yulia Rybakova,[1,2,6] Piotr S. Kowalski,[1,2,6] Yuxuan Huang,[1] John T. Gonzalez,[1] Michael W. Heartlein,[5] Frank DeRosa,[5] Derfogail Delcassian,[1,2] and Daniel G. Anderson[1,2,3,4]

[1]David H. Koch Institute for Integrative Cancer Research, Massachusetts Institute of Technology, Cambridge, MA 02142, USA; [2]Department of Chemical Engineering, Massachusetts Institute of Technology, Cambridge, MA 02142, USA; [3]Institute for Medical Engineering and Science, Massachusetts Institute of Technology, Cambridge, MA 02139, USA; [4]Harvard and MIT Division of Health Science and Technology, Massachusetts Institute of Technology, Cambridge, MA 02139, USA; [5]Translate Bio, Lexington, MA 02421, USA

Antibody-based drugs are a leading class of biologics used to treat a variety of diseases, including cancer. However, wide antibody implementation is hindered by manufacturing challenges and high production cost. Use of *in-vitro*-transcribed mRNA (IVT-mRNA) for endogenous protein expression has the potential to circumvent many of the shortcomings of antibody production and therapeutic application. Here, we describe the development of an IVT-mRNA system for *in vivo* delivery of a humanized anti-HER2 (also known as ERBB2) antibody, trastuzumab, and demonstrate its anticancer activity. We engineered the IVT-mRNA sequence to maximize expression, then formulated the IVT-mRNA into lipid-based nanoparticles (LNPs) to protect the mRNA from degradation and enable efficient *in vivo* delivery. Systemic delivery of the optimized IVT-mRNA loaded into LNPs resulted in antibody serum concentrations of 45 ± 8.6 μg/mL for 14 days after LNP injection. Further studies demonstrated an improved pharmacokinetic profile of the produced protein compared to injection of trastuzumab protein. Finally, treatment of tumor-bearing mice with trastuzumab IVT-mRNA LNPs selectively reduced the volume of HER2-positive tumors and improved animal survival. Taken together, the results of our study demonstrate that using IVT-mRNA LNPs to express full-size therapeutic antibodies in the liver can provide an effective strategy for cancer treatment and offers an alternative to protein administration.

INTRODUCTION

Antibody-based drugs are a leading class of biologics for treatment of cancer, chronic inflammation, and autoimmune diseases.[1] However, the process of large-scale antibody production has many challenges: purification protocols are complex and often have to be tailored for each individual antibody; high frequency of aberrant post-translational modifications necessitate extensive and costly quality control; mammalian antibody-producing cell lines are prone to mutations and expensive to maintain.[2–6] Furthermore, antibodies themselves are susceptible to rapid clearance and degradation by serum enzymes. In some cases, this rapid elimination requires frequent drug dosing, which additionally increases treatment cost and can lead to unwanted side effects, including immune system activation.[7]

As an alternative approach, antibodies can be produced *in vivo* by delivery of *in-vitro*-transcribed mRNA (IVT-mRNA). IVT-mRNA has demonstrated the potential to generate high levels of circulating protein *in vivo* as compared to DNA plasmids and viral vectors.[8,9] IVT-mRNA production protocol is uniform for several antibodies and does not require mammalian cell culture. Using IVT-mRNA, antibody production is transferred inside the body, allowing better control over post-translational modifications. Moreover, the process of antibody structure optimization can be simplified by using IVT-mRNA to express protein therapeutics, rather than delivering protein directly.[10] In addition, IVT-mRNA delivery allows therapeutic antibody expression within the host cell and can therefore aid in directing therapeutics toward intracellular targets. Although RNA is very unstable, the introduction of base modifications such as 5-methoxyuridine (5 moU) or N1-methyl-pseudouridine (N1Ψ) has recently been reported to improve IVT-mRNA stability and reduce the associated immunogenicity.[11–14] Finally, because there is no need for IVT-mRNA to enter the cell nucleus to be functional, the risk of insertional mutagenesis is minimized, and transfection efficacy is improved in non-dividing cells.

Currently, lipid-based nanoparticles (LNPs) are the most advanced non-viral platform for IVT-mRNA delivery to the liver. LNPs composed of ionizable lipids and lipid-like materials have demonstrated efficacy for delivery of therapeutic mRNA in both rodents and non-human primates.[15–18] By formulating mRNA into LNPs, IVT-mRNA is protected from degradation, and its transfer across cell membranes is facilitated. Besides, LNPs enable selective mRNA to the liver and facilitate the escape of IVT-mRNA from endosomal compartments into the cell cytoplasm.[19–24] Nanoparticle-formulated IVT-mRNA is therefore well suited to overcoming many difficulties associated with the production and administration of antibody-based drugs.

Received 27 March 2019; accepted 7 May 2019;
https://doi.org/10.1016/j.ymthe.2019.05.012.

[6]These authors contributed equally to this work.

Correspondence: Daniel G. Anderson, PhD, David H. Koch Institute for Integrative Cancer Research, Massachusetts Institute of Technology, Cambridge, MA 02142, USA
E-mail: dgander@mit.edu

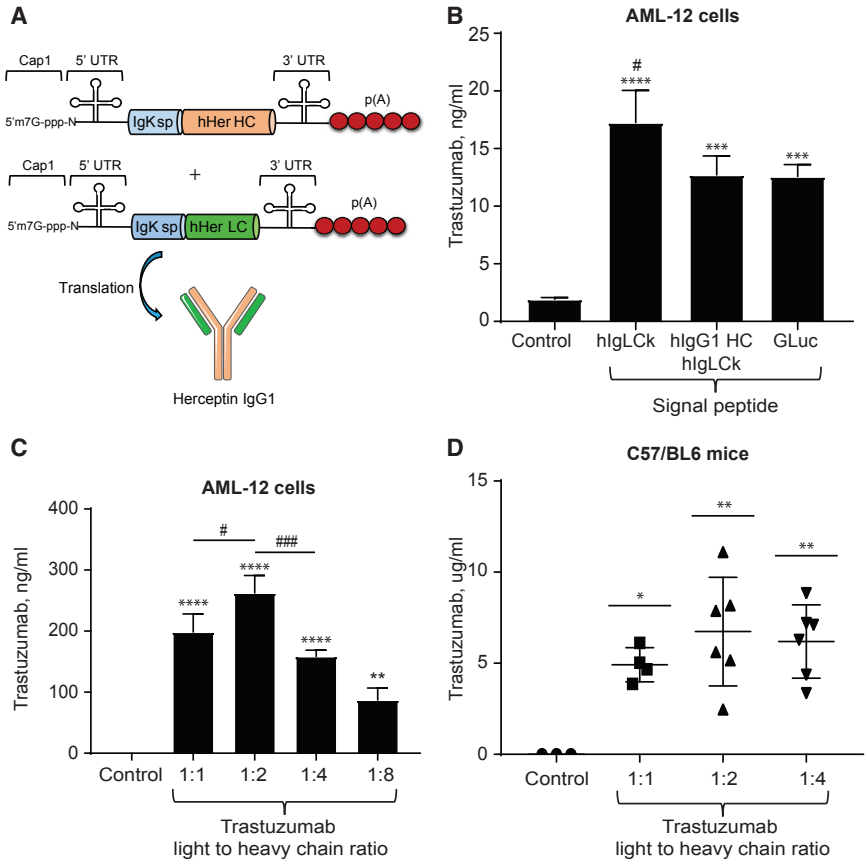

Figure 1. Optimization of the RNA Construct

(A) Schematic of mRNAs encoding the heavy (HC) and light (LC) chains of the trastuzumab. sp, signal peptide; p(A), poly A tail. (B) Trastuzumab levels (mean ± SD) in medium and lysates 24 h after AML-12 cell transfection with trastuzumab. IVT-mRNAs containing signal peptide from human immunoglobulin light chain kappa (hIgLCk), human immunoglobulin heavy chain G1 and light chain kappa (hIgG1 HC/hIgLCk) or Gaussia luciferase (GLuc). ****$p \leq 0.0001$ or ***$p \leq 0.001$ compared to control, #$p \leq 0.05$ compared to hIgG1 HC/hIgLCk SP and GLuc SP, n = 3. (C) Trastuzumab levels (mean ± SD) in AML-12 cell medium 24 h after transfection with IVT-mRNA for trastuzumab light and heavy chain at 1:1, 1:2, 1:4, or 1:8 ratio, respectively. ****$p \leq 0.0001$, ***$p \leq 0.001$ or **$p \leq 0.01$ compared to control; #$p \leq 0.05$ and ###$p \leq 0.001$, $n \geq 3$. (D) Trastuzumab levels (mean ± SD) in C57BL/6 mouse serum 24 h after injection of 0.5 mg/kg LNPs with IVT-mRNA for trastuzumab light and heavy chain in 1:1, 1:2, or 1:4 ratios. *$p \leq 0.05$, **$p \leq 0.01$, $n \geq 3$. (B–D) One-way ANOVA with Tukey's post hoc test.

Here, we describe the development of an LNP-based IVT-mRNA system for *in vivo* delivery of an anti-human epidermal growth factor receptor 2 (HER2, also known as ERBB2) antibody, trastuzumab, and demonstrate functionality of the produced protein. Trastuzumab is an antibody-based cancer drug targeting HER2,[25,26] which is overexpressed in approximately 30% of breast cancer patients.[27] The binding of trastuzumab to HER2 prevents both receptor cleavage and dimerization and results in abrogation of downstream proliferative and pro-survival pathways (reviewed by Hudis[28]). In addition, trastuzumab-induced, antibody-dependent, cell-mediated cytotoxicity has been shown to be very important in the trastuzumab antitumor effect (F. Hotaling et al., 1996, Proc. Am. Assoc. Cancer Res., abstract; S. Pegram et al., 1997, Proc. Am. Assoc. Cancer Res., abstract). Knockout of Fc receptors in mice significantly diminished the ability of trastuzumab to arrest tumor growth *in vivo*.[29]

Based on a publicly available trastuzumab amino acid sequence, we designed an IVT-mRNA sequence and codon optimized it for expression in mammalian cells. We used liver-targeting LNPs to achieve IVT-mRNA *in vivo* delivery and production of trastuzumab. We showed that optimization of signal peptide and antibody heavy-to-light-chain ratio results in an average serum trastuzumab concentration of ~40 μg/mL 24 h after injection. Furthermore, we performed pharmacodynamic and pharmacokinetic studies and demonstrated the anticancer efficacy of the expressed antibody, using *in vitro* assays and a mouse xenograft model. We showed that using IVT-mRNA LNPs to express full-size therapeutic antibody trastuzumab in the liver is an effective strategy for cancer treatment. This approach may offer an alternative to the administration of a wide range of antibody therapeutics in cancer treatment.

RESULTS

Design and Optimization of Trastuzumab mRNA for LNP Delivery

An mRNA molecule consists of a cap, 5′ and 3′ UTRs, a protein-coding sequence, and a polyA tail (Figure 1A). It has been shown that 2′-O-methylation of naturally occurring Cap 0 (Cap1) significantly enhances mRNA translation.[30] Cap 1 was therefore used for all IVT-mRNA synthesized in the study. We used a 5′ UTR consisting of a partial sequence of the cytomegalovirus (CMV) immediate early 1 (IE1) gene and 3′ UTR consisting of a partial sequence of the human growth hormone (hGH) gene. These two regions have been shown to induce efficient protein expression in different tissues *in vivo*.[24,31] A 3′ polyA tail was estimated to be approximately 120 nt long. From this basic sequence we continued RNA construct optimization by varying the signal peptide sequence and the heavy-to-light-chain ratio to improve trastuzumab expression.

The majority of secretory proteins contain a short amino acid sequence (16–30 amino acids long) at the N terminus called the signal peptide (SP) sequence. The SP is important for secretory protein translocation into the endoplasmic reticulum and the subsequent secretion of proteins from the cell. Despite substantial variation in

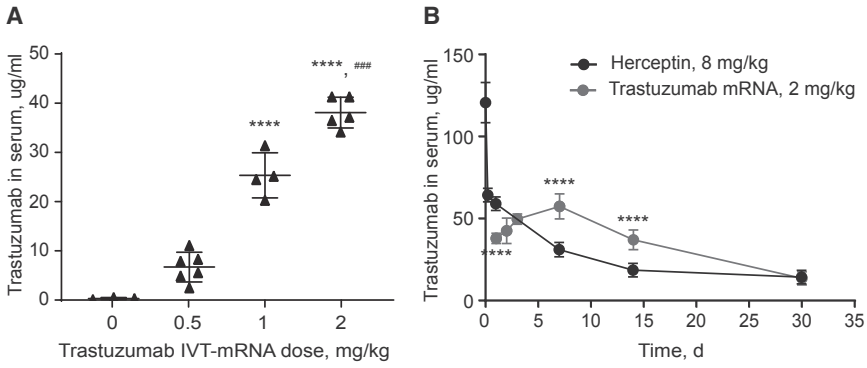

Figure 2. *In Vivo* Validation of Trastuzumab mRNA

(A) Trastuzumab concentrations in C57BL/6 mouse serum 24 h after injection of cKK-E12 LNPs with trastuzumab mRNA via the tail vein in different doses. Mean ± SD. ****p ≤ 0.0001 compared with control, ###p ≤ 0.001 compared to 1 mg/kg. (B) Pharmacokinetics of trastuzumab in C57BL/6 mouse serum after a single i.v. dose of 8 mg/kg Herceptin (Genentech) or of 2 mg/kg cKK-E12 LNPs with trastuzumab mRNA. Mean ± SD. Two-way repeated-measures ANOVA with the Sidak multiple-comparisons test was used to compare trastuzumab serum levels on day 1, 7, 14, and 30, after administration of trastuzumab mRNA versus Herceptin. ****p ≤ 0.0001, ns, p ≤ 0.05, n = 5.

SP sequences between different proteins and species, they are often functionally interchangeable. For example, in human endostatin, the replacement of native SP with Gaussia luciferase (GLuc) SP enhanced protein expression and secretion. Interestingly, in that study, GLuc SP increased protein production more than SP from human albumin or interleukin-2, which are both well-known proteins secreted at high levels in the serum.[32] Similarly, replacement of the original SP in cytokine-like 1 (CYTL1) protein with human immunoglobulin light chain kappa (hIgLCk) SP significantly increased the expression of this protein.[33] Moreover, using a bioinformatics approach based on analysis and clustering of existing human IgG1 heavy and light chain SP sequences, an H5/L1 SP combination has previously been identified and validated as the most optimal synthetic SP combination for trastuzumab production.[34]

Protein sequences for the majority of recombinant therapeutic antibodies can be found in public databases; however, these sequences often do not include an SP. To identify the most efficient SP for trastuzumab expression, we compared IVT-mRNA synthesized with GLuc, H5/L1, or hIgLCk SP (SP sequences are listed in Table S1). We used a protein sequence available at DrugBank to synthesize IVT-mRNA for trastuzumab's (trastuzumab mRNA) heavy and light chains. The protein sequence was converted into an mRNA sequence optimized for expression in mammalian cells. Trastuzumab mRNA with different SPs was then transfected into mouse hepatocytes (AML-12 cells), and trastuzumab concentrations were measured by ELISA in cell lysates and conditioned media. Although intracellular levels of trastuzumab were not affected by the SP sequence, we found that the mRNA containing hIgLCk SP resulted in higher levels of trastuzumab in the cell medium compared to GLuc and H5/L1 SPs (Figure 1B). Trastuzumab mRNA with hIgLCk SP was used in all subsequent studies.

It has been reported that protein translation rates decrease as mRNA length increases.[35,36] Since the heavy chain (HC) of human IgG1 is two times longer than the light chain (LC), we hypothesized that slower expression rates of the HC compared to the LC were limiting IgG1 assembly and secretion. We next investigated whether increasing the HC-to-LC ratio could enhance protein synthesis. We transfected AML-12 cells with trastuzumab's heavy and LC mRNA in different ratios (wt:wt): 1:1, 1:2, 1:4, and 1:8. We found that transfection using constructs containing 1:2 LC:HC resulted in significantly higher expression of trastuzumab compared to the other ratios (Figure 1C). We also observed that further increasing the LC-to-HC mRNA ratio decreased protein production, possibly because of the stoichiometric limit of LC molecules required to form a complete antibody. Surprisingly, *in vivo* we did not find a significant difference between the different ratios, although average protein expression was highest in animals injected with the 1:2 LC:HC ratio compared to the 1:1 or 1:4 ratios (Figure 1D). We chose to use an LC:HC ratio of 1:2 in all subsequent studies. The full trastuzumab sequence used in the study is presented in Figure S1.

In Vivo Validation of Trastuzumab Production

Next, we explored delivery of the optimized trastuzumab mRNA *in vivo*. For this study we used cKK-E12 (also known as MD-1) lipid-like nanoparticles that have demonstrated potent and selective small interfering RNA (siRNA) delivery to parenchymal liver cells in non-human primates[37] and high expression of EPO IVT-mRNA in rodents.[38]

To evaluate whether the optimized trastuzumab mRNA is capable of producing protein *in vivo*, we measured trastuzumab levels in mouse serum after intravenous administration of a single-dose of trastuzumab mRNA encapsulated in cKK-E12 nanoparticles. C57BL/6 mice were injected with 0.5, 1, or 2 mg/kg (based on encapsulated mRNA) of trastuzumab mRNA. All doses were well tolerated, and no adverse events were observed. As shown in Figure 2A, we found a dose-dependent increase in trastuzumab protein levels in mouse serum 24 h after administration. Upon injection with 2 mg/kg of the mRNA, approximately 40 μg trastuzumab/mL serum was produced (Figure 2A). Further monitoring revealed that trastuzumab serum concentration continued to increase during the following 7 days and reached 57.5 ± 7.6 μg/mL at 7 days after the injection (Figure 2B).

To compare the pharmacokinetic profiles of our endogenously expressed trastuzumab with the current standard of treatment (trastuzumab protein [Herceptin]), we administered a single injection of 8 mg/kg Herceptin (Genentech) to C57BL6 mice and monitored trastuzumab serum levels for 1 month. We used 8 mg/kg because it is the

Table 1. Analysis of Trastuzumab Pharmacokinetics in Mouse Serum after a Single i.v. Dose of Herceptin or Trastuzumab mRNA-LNPs

Parameter	Unit	Trastuzumab mRNA (2 mg/kg)	Herceptin (8 mg/kg)
$t_{1/2}$	h	241	251
AUC_{0-t}	μg/mL*h	28,608	17,422.7
Cl_obs	(mg/kg)/(μg/mL)/h	6.991E-05	0.0003549
Vss_obs	(mg/kg)/(μg/mL)	0.0275	0.151

Calculations were performed using PKSolver 2.0. Cl, plasma clearance; Vss, steady-state volume of distribution; $t_{1/2}$, half-life; AUC_{0-t}, the area under the curve; obs, observed.

highest Herceptin dose used in patients.[39,40] As shown in Figure 2B, 30 min after administration, 120.5 ± 12 μg/mL Herceptin antibody was detected in the serum. These levels dramatically decreased within the next few hours and reached 64 ± 4 μg/mL at 6 h after administration. One day after injection, the trastuzumab serum concentration was measured at 59 ± 4 μg/mL and continued to decrease slowly over the next few weeks. Analysis of these trastuzumab pharmacokinetics (Table 1) revealed a comparable half-life for both mRNA-LNPs and Herceptin treatment. The mRNA-based delivery resulted in a 64% higher antibody serum concentration over the course of 30 days, as reflected by the area under the curve (AUC_{0-t}). The serum clearance (Cl) and steady-state volume of distribution (Vss) were approximately 5-fold higher after injection with Herceptin than after injection of trastuzumab mRNA-LNPs.

Overall, a single dose of LNPs with IVT-mRNA encoding trastuzumab at 2 mg/kg showed favorable serum pharmacokinetics of the antibody over the course of 1 month, as compared to a single injection of Herceptin at 8 mg/kg.

Functional *In Vitro* Validation of the Optimized Trastuzumab RNA Construct

To verify the primary sequence of the protein produced upon delivery of trastuzumab mRNA-loaded LNPs, we performed mass spectrometry analysis of the IgG isolated from the mouse serum. Liquid chromatography-tandem mass spectometry (LC-MS/MS) confirmed that the primary sequence of the produced protein matched trastuzumab's amino acid sequence (Figure S2; Table S2).

To investigate whether trastuzumab produced using optimized mRNA could retain its anticancer activity, we studied its effects on breast cancer cell survival and antibody-dependent cellular cytotoxicity (ADCC). We used two HER2-positive cell lines: SKBR3 and BT-474.[41,42] Trastuzumab was isolated from the serum of mice injected with trastuzumab mRNA on a Protein A column. To control for mouse IgG binding to the column along with trastuzumab, the process was also performed on serum isolated from control mice that did not receive trastuzumab mRNA. The isolate from control mice was used as a control for the ADCC assay. Cell survival was measured using a Cell Titer Glo assay. Analysis of breast cancer cell survival after treatment with the isolated trastuzumab revealed a decrease in SK-BR-3 cell survival, as compared to the untreated control (Figure 3, black bars). We did not observe a decrease in BT-474 cell survival, which may have been due to the reduced sensitivity of BT-474 cells to the cell growth inhibitory effects of trastuzumab.

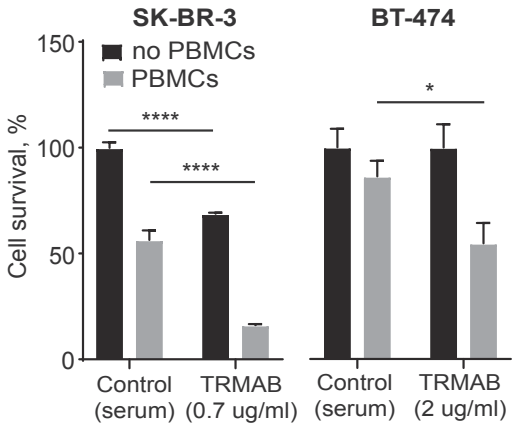

Figure 3. The ADCC Assay

Survival (mean ± SD) of HER2-positive breast cancer cells (BT-474 and SK-BR-3) after incubation with trastuzumab isolated from the serum of mice injected with 2 mg/kg trastuzumab mRNA in combination with human PBMCs. The ratio of breast cancer cells to PBMCs, 1:5. Two-way ANOVA with Tukey's post hoc test, *$p \leq 0.05$, ****$p \leq 0.0001$, n = 3.

Trastuzumab-mediated ADCC has been shown to be crucial for trastuzumab's antitumor effects. ADCC is triggered by the interaction between the antibody constant region (Fc) and the Fc-receptor present on the effector cells or on the components of the complement system. The binding of trastuzumab to HER2 receptors on the surface of target cells (HER2-positive breast cancer cells) and the subsequent recognition of the antibody Fc by effector cells results in target cell lysis. To test if mRNA-produced trastuzumab preserves its potency to induce ADCC, human peripheral blood mononuclear cells (PBMCs) were used as effector cells. We measured BT-474 and SK-BR-3 cell survival after treatment with trastuzumab isolated from mouse serum in combination with PBMCs. As shown in Figure 3 (gray bars), incubation with trastuzumab in the presence of PBMCs significantly decreased breast cancer cell survival compared with cells incubated only with PBMCs. SK-BR-3 cells were more sensitive to the treatment, most likely because of higher levels of HER2 expression.[43,44] Taken together, these data demonstrate the ability of trastuzumab produced using mRNA to induce HER2-positive breast cancer cell death via both interactions with the HER2-receptor and activation of the ADCC pathway in the presence of PBMCs.

Functional *In Vivo* Validation of the Optimized Trastuzumab mRNA Construct

To study whether trastuzumab produced using the optimized mRNA could retain its anticancer activity *in vivo*, we assessed its effects on tumor growth and animal survival in a mouse model using

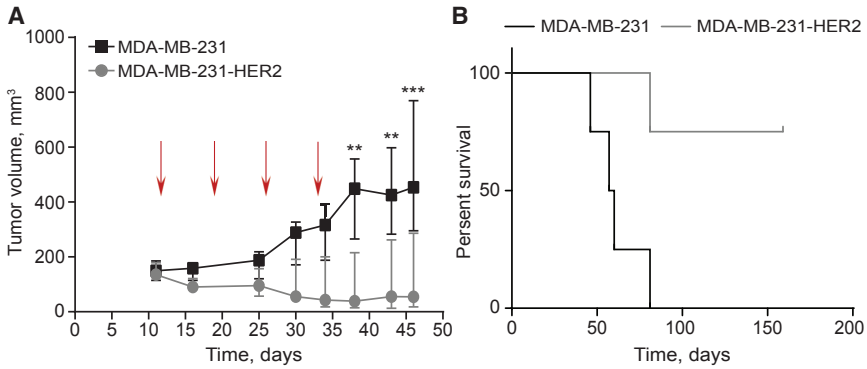

Figure 4. Investigation of the *In Vivo* Effects of Trastuzumab Therapy

(A) Growth (median ± interquartile range [IQR]) of HER2-negative (MDA-MB-231) and HER2-positive (MDA-MB-231-HER2) tumors in mice treated with the trastuzumab mRNA. Arrows indicate the days of mRNA-LNP injections. Two-way repeated-measures ANOVA with the Sidak multiple-comparisons test, $^{**}p \leq 0.01$, $^{***}p \leq 0.001$, compared with the volume of HER2-negative tumors, n = 5. (B) Kaplan-Meier analysis of animal survival after treatment with trastuzumab mRNA. Log-rank test, p = 0.0169, n = 4.

HER2-positive and -negative human breast cancer xenografts. The MDA-MB-231 cell line is HER2-negative and therefore is insensitive to trastuzumab. We transduced MDA-MB-231 cells with a human HER2-expressing plasmid to create an MDA-MB-231-HER2 cell line sensitive to trastuzumab. HER2 expression was confirmed by qPCR (Figure S3). The HER2-negative cell line was used to control for non-specific side effects associated with RNA, such as production of inflammatory cytokines (TNFa, IL-12, IL-8, and type I interferons) after RNA recognition by innate immune receptors (TLR3, TLR7, TLR8, RIG-I, MDA5, and others) and triggering of antitumor immune response via mechanisms independent of the RNA sequence.[11,45,46] In addition, these two cell lines allow us to assess HER2-specific efficacy of trastuzumab mRNA.

We have previously demonstrated that IVT-mRNA from cKK-E12 LNPs is predominantly translated in the liver with minimal translation in the spleen.[38] However, tumors often have abnormal blood supply because of high vascular permeability and ineffective lymphatic drainage. This phenomenon can lead to nanoparticle accumulation and retention (reviewed in Nagy et al.[47] and Kanasty et al.[48]). To evaluate whether cKK-E12 LNPs deliver IVT-mRNA to xenografts, we injected xenograft-bearing mice with 2 mg/kg firefly luciferase (FLuc) IVT-mRNA formulated into cKK-E12 LNPs and measured bioluminescence levels, using IVIS (Figure S4). Whole-body IVIS showed that 6 h after the injection, LNPs accumulated mainly in the liver (Figure S4A). Analysis of organs excised from athymic nude mice xenografted with MDA-MB-231-HER2 cells revealed that a bioluminescent signal was also present in tumors (Figure S4B and S4C).

To study the effects of trastuzumab mRNA on tumor growth, mice with established MDA-MB-231 or MDA-MB-231-HER2 xenografts were treated with weekly injections of 2 mg/kg trastuzumab mRNA LNPs for 4 weeks and xenograft growth was monitored (Figure 4A). At the beginning of treatment, tumor volume in both groups was ~150 mm^3 (Figure 4A, day 11). We found a significant delay in HER2-positive tumor growth compared to HER2-negative tumors (Figure 4A). One week after the final injection the average volume of HER2-positive tumors was ~100 mm^3, whereas HER2-negative xenografts were, on average, four times larger (Figure 4A, day 38). Calculation of survival fractions using the Kaplan-Meier method revealed that the treated mice with HER2-positive tumors had significantly longer morbidity-free survival (p = 0.0169, log-rank test) compared to the treated mice with HER2-negative tumors. One mouse in each group gnawed their tumors, and they were removed from the survival study.

In addition, we studied whether the trastuzumab mRNA injections, per se, can contribute to the tumor growth reduction. Mice with HER2-negative tumors were treated with saline, and the tumor growth was monitored (Figure S6A). When we compared those mice with those treated with the trastuzumab mRNA, we observed no difference in tumor growth between the two groups. Finally, to compare the antitumor effects of the trastuzumab mRNA and Herceptin, mice with HER2-positive tumors received one injection of 8 mg/kg Herceptin or saline per week for 4 weeks (Figure S6B). Although we did not observe a significant difference, the average tumor volume in mice treated with Herceptin was lower than in mice treated with saline. The low efficacy of Herceptin in our study may have been the result of infrequent injections, as we administered Herceptin only once a week instead of the standard two times per week. Importantly, when compared to mice treated with the trastuzumab mRNA, we still observed a significant reduction in tumor growth compared to saline. In addition, the average tumor volume in mice treated with the mRNA was lower than in mice treated with Herceptin.

Toxicity was evaluated 1 week after the final injection by analyzing blood and organs. Blood count revealed an approximately 2-fold decrease in lymphocyte levels in all tumor-bearing mice, which may have been associated with tumor formation (Table S3). We also observed slight variations in several serum chemistry parameters, but the changes were less than 2-fold (Table S4). Importantly, no significant changes in liver enzymes were found after 4 weeks of treatment with the LNPs, as compared to the untreated tumor-bearing mice. Histological analysis did not reveal any morphological changes in the liver and spleen of treated mice (Figure S5). Together, the data suggest that treatment with trastuzumab mRNA LNPs significantly delayed the growth of HER2-positive breast cancer in athymic nude mice, with no apparent toxicity.

DISCUSSION

In recent years, RNA therapeutics have been broadly used in a variety of clinical applications, including vaccines, protein replacement therapies, and gene editing technologies. Therapeutic anticancer vaccines designed to target tumor-associated antigens and mobilize T cell responses are being currently evaluated in the clinic (reviewed in Pastor et al.,[49] Sahn and Türeci,[50] and Kowalski et al.[51]). The use of IVT-mRNA for the initiation of endogenous antibody expression can overcome the challenges associated with the manufacture and delivery of highly demanded monoclonal-antibody-based drugs.[52,53] Specifically, the use of LNP-formulated IVT-mRNA, rather than protein, can address the limitations found with bi-specific antibodies, such as short serum half-life, manufacturing challenges, and the requirement for repeated administration.[52] In addition, using host translational machinery for continuous expression of high levels of properly folded and modified proteins makes mRNA-based antibody production simple and cost effective compared to protein-based therapeutics.[53] Furthermore, the use of IVT-mRNA simplifies the process of antibody structure optimization and enables localized antibody expression that is unavailable for conventional therapeutics.[10]

Prior efforts to use monoclonal mRNA for endogenous antibody expression have been mainly situated at the level of passive antiviral immunization.[10,53,54] In our study, we broaden application of mRNA-based delivery for monoclonal antibody production to treatment of solid tumors. We designed and optimized an IVT-mRNA delivery system for potent *in vitro* and *in vivo* expression of trastuzumab. Trastuzumab is a widely used and successful anticancer monoclonal antibody, with a well-understood mechanism of action. We developed a strategy for the rational design of an IVT-mRNA structure to maximize antibody production. Further, we demonstrated that this optimization can significantly improve *in vivo* trastuzumab protein expression, maintain both HER2 specificity and ADCC functionality, and extend survival of animals with HER2-positive breast cancer.

We identified hIgLCk as the most efficient signal peptide and optimized the antibody light-to-heavy-chain ratio to obtain maximal trastuzumab expression upon liver delivery in mice. We also demonstrated improved trastuzumab pharmacokinetics when produced using IVT-mRNA compared to Herceptin and confirmed that trastuzumab isolated from mouse serum maintained both HER2 specificity and ADCC functionality.

Mice injected with 2 mg/kg (40 μg per animal) of trastuzumab mRNA demonstrated serum levels comparable with injection of the highest clinically relevant protein dose (8 mg/kg, 160 μg per animal).[39,40] Notably, in our study, we observed potent protein expression and longer antibody persistence in mouse serum after delivery of trastuzumab mRNA, compared to previously published studies.[52–54] After delivery of 40 μg mRNA-LNPs or 160 μg protein, we demonstrated that the serum concentration of endogenously produced trastuzumab is at 24 h, comparable with the levels of the injected antibody. Moreover, trastuzumab levels in mice that received Herceptin continued to decline, while trastuzumab levels in mice injected with mRNA-LNP remained within 45 ± 8.6 μg/mL for 14 days. In fact, 2 weeks after mRNA injection, trastuzumab serum levels were still above 10 μg/mL, which is considered the minimum therapeutic plasma concentration needed for antiproliferative effects.[40] These data also support findings from previous studies,[52,53] where administration of mRNA-based drugs resulted in similar or higher antibody plasma levels compared to the corresponding purified antibody. The differences in peak concentrations may be a result of differences in the antibody sequence and delivery method. In general, plasma levels of the endogenously translated antibodies tend to be sustained longer than levels of the protein. Extended plasma circulation time in our study compared to the previously published studies using the mRNA-based approach[52,53] can be a result of differences in antibody sequence or mechanism of action. The standard administration protocol for trastuzumab in mice requires injections of 1–10 mg/kg of the protein twice a week. We showed that a prolonged presence of the endogenously expressed therapeutic antibody in the plasma has the potential to reduce administration frequency, dosing, and, subsequently, treatment cost.

Finally, our study is the first demonstration of the inhibition of solid tumor growth by a full-size antibody produced in the liver upon delivery of IVT-mRNA formulated into LNPs. We did not observe any toxic effects during our treatment regimen. *In vivo* validation of anticancer activity showed that weekly intravenous (i.v.) administration of 2 mg/kg of trastuzumab mRNA LNPs for 4 weeks inhibited breast cancer growth in athymic nude mice and improved animal survival, thus outperforming the standard of treatment, Herceptin. Importantly, we demonstrated that the inhibition of tumor growth was specific to HER2 receptor presence in the tumor cells by using MDA-MB-231 and MDA-MB-231-HER2 xenografts. Interestingly, we found that LNPs can deliver IVT-mRNA directly to the tumor. Expression of therapeutic antibodies within the tumor microenvironment or directly in tumor cells can potentially enhance therapeutic efficacy and reduce off-target effects.

In summary, our study demonstrates that using IVT-mRNA loaded into LNPs to express full-size therapeutic antibodies, such as trastuzumab, in the liver can provide an effective strategy for cancer treatment and offers an alternative to protein administration. This study also provides a guideline for the optimization of an IVT-mRNA construct, which can be used for the development of other monoclonal antibody mRNA therapies.

MATERIALS AND METHODS

Cell Culture

The mouse hepatocytes AML-12 and the human HER-positive breast carcinoma cells BT-474 and MDA-MB-231 were obtained from ATCC. SK-BR-3 cell line was a gift from the Hammond Lab (MIT). MDA-MB-231 cells expressing human HER2 (MDA-MB-231-HER2) were created in our lab. AML-12 cells were grown in a 1:1 mixture of DMEM and Ham's F12 with Insulin-Transferrin-Selenium (ITS-G) medium supplement, 100 U/mL penicillin-streptomycin (Pen/Strep), and 10% fetal bovine serum (FBS) (Gibco). The BT-474 cells were

cultured in ATCC Hybri-Care Medium supplemented with 1.5 g/L sodium bicarbonate, 100 U/mL Pen/Strep, and 10% FBS. MDA-MB-231, MDA-MB-231-HER2, and SK-BR-3 cells were grown in DMEM with 100 U/mL Pen/Strep and 10% FBS. All cell lines were cultured at 37°C in 5% CO_2. When the cells reached 70%–80% monolayer, they were detached from the flask using 0.25% Trypsin-EDTA solution and split 1:5.

Mice

All animal studies were approved by the MIT Institutional Animal Care and Use Committee and were consistent with local, state, and federal regulations, as applicable. RNA/LNPs (0.5–2 mg/kg) were administered to female C57BL/6 mice (20–25 g; Charles River Laboratories) or to female athymic nude mice (20–22 g Charles River Laboratories) intravenously via tail vein injection. Mouse blood was collected from the lateral tail vein or the submandibular vein in a sterile 1.5 mL microcentrifuge tube, incubated on ice for 10 min, and centrifuged at 2,000 *g* for 20 min at 4°C. Supernatants (serum) were collected and used for ELISA or protein isolation.

Mouse Xenograft Models

Athymic nude mice (female, aged 7–8 weeks) received subcutaneous implants in the right flank of 4×10^6 MDA-MB-231 or MDA-MB-231-HER2 cells in Dulbecco's PBS (DPBS)-Matrigel (v/v, 1:1). Treatment was started 11 days later, when xenografts reached 100–200 mm^3. Both groups of mice received one i.v. injection of 2 mg/kg trastuzumab mRNA per week for 4 weeks, formulated into cKK-E12 nanoparticles. Tumors were measured with a digital caliper, and volumes were calculated by the formula tumor volume (mm^3) = length (mm) × (width [mm])^2/2. Termination criteria were a tumor volume of 1,000 mm^3 or weight loss of 20%.

Protein Isolation

Trastuzumab was isolated from mouse blood using the Pierce Protein A IgG Purification Kit according to the manufacturer's instructions. Briefly, mouse serum was diluted with the Protein A Binding Buffer 1:1 and applied to the equilibrated Protein A column. Then, the column was washed by adding 10–15 mL of Binding Buffer. The bound IgG was eluted with 5 mL of the IgG Elution Buffer. Ultracel-10K centrifugal filters (Millipore) were used to substitute the Binding Buffer with PBS and concentrate the eluent. Trastuzumab concentration in the eluent was measured using ELISA.

In Vitro ADCC Assay

Buffy coats collected from human peripheral blood were purchased from Research Blood Components, LLC (Brighton, MA, USA) and PBMCs were isolated by density gradient centrifugation. Briefly, buffy coats were diluted 1:1 in RPMI-1640 and carefully layered over a sterile, endotoxin tested (<0.12 EU/mL) solution of Ficoll Paque Plus (density 1.007 g/mL; GE Healthcare). Layered solutions were centrifuged at 500 *g* for 40 m at room temperature to sediment unwanted cells, and the interfacial layer of PBMCs was manually isolated. PMBCs were then washed twice in RPMI-1640 before further use. After they were washed with the RPMI-1640 cell culture medium (Gibco), the cells were immediately subjected to ADCC or frozen, using Gibco Recovery Cell Culture Freezing Medium. BT-474 and SK-BR-3 cells were seeded in a 96-well plate at 15,000 cells per well and incubated overnight. The next day, 50 μL trastuzumab was added to the plates and incubated for 30 min to allow opsonization. After incubation, 50 μL of PBMCs were added to each well in 1:2, 1:5, or 1:10 ratio. The PBMCs were removed from the wells 72 h later by washing with 100 μL DPBS (Gibco). The number of survived breast cancer cells was measured by using the Cell Titer Glo assay.

Statistical Analysis

One-way ANOVA followed by Tukey's post hoc test was used for multiple-comparisons analysis. Two-way ANOVA followed by the Sidak multiple-comparisons test was used for analysis of repeated measures. The GraphPad Prism 7 package was used.

SUPPLEMENTAL INFORMATION

Supplemental Information can be found online at https://doi.org/10.1016/j.ymthe.2019.05.012.

AUTHOR CONTRIBUTIONS

Y.R. designed the study, executed the experiments, analyzed the data, and wrote the manuscript; P.S.K. was responsible for the mRNA design, synthesis, and delivery and edited the manuscript; Y.H. and J.T.G. assisted with the experiments; M.W.H. and F.D. contributed to the mRNA design and edited the manuscript; D.D. contributed to the ADCC experimental design and execution and edited the manuscript; and D.G.A. supervised the study and edited the manuscript.

CONFLICTS OF INTEREST

D.G.A., P.S.K., and Y.R. filed a patent for the design and development of the trastuzumab mRNA delivery system. The remaining authors declare no competing interests.

ACKNOWLEDGMENTS

This work was supported by Translate Bio (Lexington, MA, USA), the MIT Skoltech Initiative, Defense Advanced Research Projects Agency (W32P4Q-13-1-001), S. Leslie Misrock Frontier Research Fund for Cancer Nanotechnology, Juvenile Diabetes Research Foundation (JDRF) postdoctoral fellowship grant 3-PDF-2017-383-A-N, and a Koch Institute Support (core) grant P30-CA14051 from the National Cancer Institute. We thank the Koch Institute Swanson Biotechnology Center for technical support, specifically the Animal Imaging and Preclinical Testing Core, the Histology Core, and the Biopolymers and Proteomics Core. We also thank Prof. Oliver Jonas (Brigham and Women's Hospital) and Dr. Marion Paolini (MIT), who provided insight into the development of a HER2-positive breast cancer model, and Dr. Kevin McHugh (MIT) for comments that improved the manuscript.

REFERENCES

1. Urquhart, L. (2018). Market watch: Top drugs and companies by sales in 2017. Nat. Rev. Drug Discov. *17*, 232.

2. Samaranayake, H., Wirth, T., Schenkwein, D., Räty, J.K., and Ylä-Herttuala, S. (2009). Challenges in monoclonal antibody-based therapies. Ann. Med. *41*, 322–331.
3. Kunert, R., and Reinhart, D. (2016). Advances in recombinant antibody manufacturing. Appl. Microbiol. Biotechnol. *100*, 3451–3461.
4. Chusainow, J., Yang, Y.S., Yeo, J.H., Toh, P.C., Asvadi, P., Wong, N.S., and Yap, M.G. (2009). A study of monoclonal antibody-producing CHO cell lines: what makes a stable high producer? Biotechnol. Bioeng. *102*, 1182–1196.
5. Li, F., Vijayasankaran, N., Shen, A.Y., Kiss, R., and Amanullah, A. (2010). Cell culture processes for monoclonal antibody production. MAbs *2*, 466–479.
6. Van Hoecke, L., and Roose, K. (2019). How mRNA therapeutics are entering the monoclonal antibody field. J. Transl. Med. *17*, 54.
7. Awwad, S., and Angkawinitwong, U. (2018). Overview of antibody drug delivery. Pharmaceutics *10*, 1–24.
8. Zangi, L., Lui, K.O., von Gise, A., Ma, Q., Ebina, W., Ptaszek, L.M., Später, D., Xu, H., Tabebordbar, M., Gorbatov, R., et al. (2013). Modified mRNA directs the fate of heart progenitor cells and induces vascular regeneration after myocardial infarction. Nat. Biotechnol. *31*, 898–907.
9. Mahiny, A.J., Dewerth, A., Mays, L.E., Alkhaled, M., Mothes, B., Malaeksefat, E., Loretz, B., Rottenberger, J., Brosch, D.M., Reautschnig, P., et al. (2015). In vivo genome editing using nuclease-encoding mRNA corrects SP-B deficiency. Nat. Biotechnol. *33*, 584–586.
10. Tiwari, P.M., Vanover, D., Lindsay, K.E., Bawage, S.S., Kirschman, J.L., Bhosle, S., Lifland, A.W., Zurla, C., and Santangelo, P.J. (2018). Engineered mRNA-expressed antibodies prevent respiratory syncytial virus infection. Nat. Commun. *9*, 3999.
11. Karikó, K., Buckstein, M., Ni, H., and Weissman, D. (2005). Suppression of RNA recognition by Toll-like receptors: the impact of nucleoside modification and the evolutionary origin of RNA. Immunity *23*, 165–175.
12. Holtkamp, S., Kreiter, S., Selmi, A., Simon, P., Koslowski, M., Huber, C., Türeci, O., and Sahin, U. (2006). Modification of antigen-encoding RNA increases stability, translational efficacy, and T-cell stimulatory capacity of dendritic cells. Blood *108*, 4009–4017.
13. Andries, O., Mc Cafferty, S., De Smedt, S.C., Weiss, R., Sanders, N.N., and Kitada, T. (2015). N(1)-methylpseudouridine-incorporated mRNA outperforms pseudouridine-incorporated mRNA by providing enhanced protein expression and reduced immunogenicity in mammalian cell lines and mice. J. Control. Release *217*, 337–344.
14. Li, B., Luo, X., and Dong, Y. (2016). Effects of Chemically Modified Messenger RNA on Protein Expression. Bioconjug. Chem. *27*, 849–853.
15. Kauffman, K.J., Dorkin, J.R., Yang, J.H., Heartlein, M.W., DeRosa, F., Mir, F.F., Fenton, O.S., and Anderson, D.G. (2015). Optimization of Lipid Nanoparticle Formulations for mRNA Delivery in Vivo with Fractional Factorial and Definitive Screening Designs. Nano Lett. *15*, 7300–7306.
16. DeRosa, F., Guild, B., Karve, S., Smith, L., Love, K., Dorkin, J.R., Kauffman, K.J., Zhang, J., Yahalom, B., Anderson, D.G., and Heartlein, M.W. (2016). Therapeutic efficacy in a hemophilia B model using a biosynthetic mRNA liver depot system. Gene Ther. *23*, 699–707.
17. Sabnis, S., Kumarasinghe, E.S., Salerno, T., Mihai, C., Ketova, T., Senn, J.J., Lynn, A., Bulychev, A., McFadyen, I., Chan, J., et al. (2018). A Novel Amino Lipid Series for mRNA Delivery: Improved Endosomal Escape and Sustained Pharmacology and Safety in Non-human Primates. Mol. Ther. *26*, 1509–1519.
18. Ramaswamy, S., Tonnu, N., Tachikawa, K., Limphong, P., Vega, J.B., Karmali, P.P., Chivukula, P., and Verma, I.M. (2017). Systemic delivery of factor IX messenger RNA for protein replacement therapy. Proc. Natl. Acad. Sci. USA *114*, E1941–E1950.
19. Sahin, U., Karikó, K., and Türeci, Ö. (2014). mRNA-based therapeutics–developing a new class of drugs. Nat. Rev. Drug Discov. *13*, 759–780.
20. Yin, H., Kanasty, R.L., Eltoukhy, A.A., Vegas, A.J., Dorkin, J.R., and Anderson, D.G. (2014). Non-viral vectors for gene-based therapy. Nat. Rev. Genet. *15*, 541–555.
21. Kauffman, K.J., Webber, M.J., and Anderson, D.G. (2016). Materials for non-viral intracellular delivery of messenger RNA therapeutics. J. Control. Release *240*, 227–234.
22. Hajj, K.A., and Whitehead, K.A. (2017). Tools for translation: Non-viral materials for therapeutic mRNA delivery. Nat. Rev. Mater. *2*, 17056.
23. Guan, S., and Rosenecker, J. (2017). Nanotechnologies in delivery of mRNA therapeutics using nonviral vector-based delivery systems. Gene Ther. *24*, 133–143.
24. Kowalski, P.S., Capasso Palmiero, U., Huang, Y., Rudra, A., Langer, R., and Anderson, D.G. (2018). Ionizable Amino-Polyesters Synthesized via Ring Opening Polymerization of Tertiary Amino-Alcohols for Tissue Selective mRNA Delivery. Adv. Mater. *30*, e1801151.
25. Hudziak, R.M., Lewis, G.D., Winget, M., Fendly, B.M., Shepard, H.M., and Ullrich, A. (1989). p185HER2 monoclonal antibody has antiproliferative effects in vitro and sensitizes human breast tumor cells to tumor necrosis factor. Mol. Cell. Biol. *9*, 1165–1172.
26. Carter, P., Presta, L., Gorman, C.M., Ridgway, J.B., Henner, D., Wong, W.L., Rowland, A.M., Kotts, C., Carver, M.E., and Shepard, H.M. (1992). Humanization of an anti-p185HER2 antibody for human cancer therapy. Proc. Natl. Acad. Sci. USA *89*, 4285–4289.
27. Cancer Genome Atlas Network (2012). Comprehensive molecular portraits of human breast tumours. Nature *490*, 61–70.
28. Hudis, C.A. (2007). Trastuzumab: mechanism of action and use in clinical practice. N. Engl. J. Med. *357*, 39–51.
29. Clynes, R.A., Towers, T.L., Presta, L.G., and Ravetch, J.V. (2000). Inhibitory Fc receptors modulate in vivo cytotoxicity against tumor targets. Nat. Med. *6*, 443–446.
30. Kuge, H., Brownlee, G.G., Gershon, P.D., and Richter, J.D. (1998). Cap ribose methylation of c-mos mRNA stimulates translation and oocyte maturation in Xenopus laevis. Nucleic Acids Res. *26*, 3208–3214.
31. Kauffman, K.J., Mir, F.F., Jhunjhunwala, S., Kaczmarek, J.C., Hurtado, J.E., Yang, J.H., Webber, M.J., Kowalski, P.S., Heartlein, M.W., DeRosa, F., and Anderson, D.G. (2016). Efficacy and immunogenicity of unmodified and pseudouridine-modified mRNA delivered systemically with lipid nanoparticles in vivo. Biomaterials *109*, 78–87.
32. Knappskog, S., Ravneberg, H., Gjerdrum, C., Trösse, C., Stern, B., and Pryme, I.F. (2007). The level of synthesis and secretion of Gaussia princeps luciferase in transfected CHO cells is heavily dependent on the choice of signal peptide. J. Biotechnol. *128*, 705–715.
33. Wang, X., Liu, H., Yuan, W., Cheng, Y., and Han, W. (2016). Efficient production of CYTL1 protein using mouse IgGκ signal peptide in the CHO cell expression system. Acta Biochim. Biophys. Sin. (Shanghai) *48*, 391–394.
34. Haryadi, R., Ho, S., Kok, Y.J., Pu, H.X., Zheng, L., Pereira, N.A., Li, B., Bi, X., Goh, L.T., Yang, Y., and Song, Z. (2015). Optimization of heavy chain and light chain signal peptides for high level expression of therapeutic antibodies in CHO cells. PLoS ONE *10*, e0116878.
35. Arava, Y., Wang, Y., Storey, J.D., Liu, C.L., Brown, P.O., and Herschlag, D. (2003). Genome-wide analysis of mRNA translation profiles in Saccharomyces cerevisiae. Proc. Natl. Acad. Sci. USA *100*, 3889–3894.
36. Valleriani, A., Zhang, G., Nagar, A., Ignatova, Z., and Lipowsky, R. (2011). Length-dependent translation of messenger RNA by ribosomes. Phys. Rev. E Stat. Nonlin. Soft Matter Phys. *83*, 042903.
37. Dong, Y., Love, K.T., Dorkin, J.R., Sirirungruang, S., Zhang, Y., Chen, D., Bogorad, R.L., Yin, H., Chen, Y., Vegas, A.J., et al. (2014). Lipopeptide nanoparticles for potent and selective siRNA delivery in rodents and nonhuman primates. Proc. Natl. Acad. Sci. USA *111*, 3955–3960.
38. Fenton, O.S., Kauffman, K.J., Kaczmarek, J.C., McClellan, R.L., Jhunjhunwala, S., Tibbitt, M.W., Zeng, M.D., Appel, E.A., Dorkin, J.R., Mir, F.F., et al. (2017). Synthesis and Biological Evaluation of Ionizable Lipid Materials for the In Vivo Delivery of Messenger RNA to B Lymphocytes. Adv. Mater. *29*, 1–7.
39. Goldenberg, M.M. (1999). Trastuzumab, a recombinant DNA-derived humanized monoclonal antibody, a novel agent for the treatment of metastatic breast cancer. Clin. Ther. *21*, 309–318.
40. Leyland-Jones, B., Arnold, A., Gelmon, K., Verma, S., Ayoub, J.P., Seidman, A., Dias, R., Howell, J., and Rakhit, A. (2001). Pharmacologic insights into the future of trastuzumab. Ann. Oncol. *12* (*Suppl 1*), S43–S47.
41. Holliday, D.L., and Speirs, V. (2011). Choosing the right cell line for breast cancer research. Breast Cancer Res. 13–215.

42. Dai, X., Cheng, H., Bai, Z., and Li, J. (2017). Breast Cancer Cell Line Classification and Its Relevance with Breast Tumor Subtyping. J. Cancer *8*, 3131–3141.

43. Subik, K., Lee, J.F., Baxter, L., Strzepek, T., Costello, D., Crowley, P., Xing, L., Hung, M.C., Bonfiglio, T., Hicks, D.G., and Tang, P. (2010). The Expression Patterns of ER, PR, HER2, CK5/6, EGFR, Ki-67 and AR by Immunohistochemical Analysis in Breast Cancer Cell Lines. Breast Cancer (Auckl.) *4*, 35–41.

44. Pasleau, F., Grooteclaes, M., and Gol-Winkler, R. (1993). Expression of the c-erbB2 gene in the BT474 human mammary tumor cell line: measurement of c-erbB2 mRNA half-life. Oncogene *8*, 849–854.

45. Karikó, K., Ni, H., Capodici, J., Lamphier, M., and Weissman, D. (2004). mRNA is an endogenous ligand for Toll-like receptor 3. J. Biol. Chem. *279*, 12542–12550.

46. Lee, S., and Margolin, K. (2011). Cytokines in cancer immunotherapy. Cancers (Basel) *3*, 3856–3893.

47. Nagy, J.A., Chang, S.-H., Dvorak, A.M., and Dvorak, H.F. (2009). Why are tumour blood vessels abnormal and why is it important to know? Br. J. Cancer *100*, 865–869.

48. Kanasty, R., Dorkin, J.R., Vegas, A., and Anderson, D. (2013). Delivery materials for siRNA therapeutics. Nat. Mater. *12*, 967–977.

49. Pastor, F., Berraondo, P., Etxeberria, I., Frederick, J., Sahin, U., Gilboa, E., and Melero, I. (2018). An RNA toolbox for cancer immunotherapy. Nat. Rev. Drug Discov. *17*, 751–767.

50. Sahin, U., and Türeci, Ö. (2018). Personalized Vaccines for Cancer Immunotherapy. Science *359*, 1355–1360.

51. Kowalski, P.S., Rudra, A., Miao, L., and Anderson, D.G. (2019). Delivering the Messenger: Advances in Technologies for Therapeutic mRNA Delivery. Mol. Ther. *27*, 710–728.

52. Stadler, C.R., Bähr-Mahmud, H., Celik, L., Hebich, B., Roth, A.S., Roth, R.P., Karikó, K., Türeci, Ö., and Sahin, U. (2017). Elimination of large tumors in mice by mRNA-encoded bispecific antibodies. Nat. Med. *23*, 815–817.

53. Pardi, N., Secreto, A.J., Shan, X., Debonera, F., Glover, J., Yi, Y., Muramatsu, H., Ni, H., Mui, B.L., Tam, Y.K., et al. (2017). Administration of nucleoside-modified mRNA encoding broadly neutralizing antibody protects humanized mice from HIV-1 challenge. Nat. Commun. *8*, 14630.

54. Thran, M., Mukherjee, J., Pönisch, M., Fiedler, K., Thess, A., Mui, B.L., Hope, M.J., Tam, Y.K., Horscroft, N., Heidenreich, R., et al. (2017). mRNA mediates passive vaccination against infectious agents, toxins, and tumors. EMBO Mol. Med. *9*, 1434–1447.

YMTHE, Volume *27*

Supplemental Information

mRNA Delivery for Therapeutic Anti-HER2 Antibody Expression *In Vivo*

Yulia Rybakova, Piotr S. Kowalski, Yuxuan Huang, John T. Gonzalez, Michael W. Heartlein, Frank DeRosa, Derfogail Delcassian, and Daniel G. Anderson

SUPPLEMENTAL MATERIALS

Supplemental Figure 1. *Full trastuzumab construct used in the study.*

human immunoglobulin light chain kappa signal peptide

protein coding sequence without signal peptide

Trastuzumab heavy chain mRNA

GGACAGATCGCCTGGAGACGCCATCCACGCTGTTTTGACCTCCATAGAAGACACCG
GGACCGATCCAGCCTCCGCGGCCGGGAACGGTGCATTGGAACGCGGATTCCCCGTG
CCAAGAGTGACTCACCGTCCTTGACACGATGAGGGCTTGGATCTTCTTTCTGCTCTG
CCTGGCCGGGCGCGCCTTGGCCGAAGTTCAACTGGTAGAGAGTGGAGGTGGGCTTG
TGCAACCAGGCGGATCCTTGCGACTGTCCTGCGCCGCTTCAGGCTTCAACATCAAGG
ACACCTACATCCATTGGGTCCGCCAGGCACCAGGAAAAGGTCTTGAATGGGTGGCC
AGAATCTACCCTACTAACGGTTACACCAGATATGCAGACTCCGTTAAGGGGCGATTT
ACCATTTCAGCAGACACCTCTAAGAACACCGCTTACCTGCAGATGAACTCACTTCGA
GCTGAGGACACCGCCGTTTACTATTGCAGCAGATGGGGCGGTGACGGCTTCTACGCT
ATGGATTACTGGGGACAGGGGACTTTGGTAACTGTGAGTAGTGCATCTACAAAGGG
GCCAAGCGTGTTCCCACTTGCCCCATCTTCTAAAAGCACCTCAGGAGGGACTGCAGC
CTTGGGTTGCTTGGTTAAAGATTATTTTCCAGAGCCTGTAACTGTATCCTGGAATAGT
GGGGCCCTCACAAGCGGAGTACATACTTTCCCTGCAGTATTGCAGTCTAGTGGACTC
TACTCTCTCAGCAGTGTAGTGACCGTACCTTCCAGTTCACTTGGAACACAGACCTAT
ATTTGCAATGTGAATCATAAGCCATCTAATACTAAAGTGGATAAGAAAGTGGAGCC
TAAATCTTGTGACAAGACTCATACATGCCCTCCCTGCCCTGCCCCTGAACTGTTGGG
AGGGCCCTCTGTATTTCTCTTCCCCCCTAAACCAAAGGACACCCTGATGATCAGTCG
AACTCCTGAGGTGACTTGTGTGGTTGTTGACGTGTCACATGAGGATCCCGAAGTGAA
ATTCAACTGGTACGTCGATGGAGTAGAGGTACACAATGCAAAGACAAAACCTAGGG
AGGAACAGTATAATTCTACCTATAGAGTGGTGTCTGTTCTCACAGTTCTCCATCAAG
ACTGGTTGAACGGTAAAGAATATAAATGCAAAGTCTCCAATAAGGCTTTGCCCGCTC
CCATTGAAAAAACAATCAGTAAAGCCAAAGGCCAGCCACGCGAACCACAGGTCTAC
ACCCTTCCACCATCTCGCGAAGAAATGACTAAGAATCAAGTGTCACTCACATGCCTC
GTCAAGGGCTTTTACCCTTCTGATATTGCAGTTGAATGGGAGTCTAACGGGCAGCCC
GAGAATAATTACAAGACTACCCCCCCCGTCCTTGACTCTGATGGCAGCTTTTTCCTGT
ACTCAAAATTGACTGTGGACAAGTCTCGATGGCAACAGGGTAATGTTTTCTCCTGTA
GCGTAATGCACGAGGCTCTTCATAACCATTATACCCAAAAATCTCTTTCATTGTCCCC
TGGAAAATGACGGGTGGCATCCCTGTGACCCCTCCCCAGTGCCTCTCCTGGCCCTGG
AAGTTGCCACTCCAGTGCCCACCAGCCTTGTCCTAATAAAATTAAGTTGCATCAAGC
T

Trastuzumab light chain mRNA

GGACAGATCGCCTGGAGACGCCATCCACGCTGTTTTGACCTCCATAGAAGACACCG
GGACCGATCCAGCCTCCGCGGCCGGGAACGGTGCATTGGAACGCGGATTCCCCGTG
CCAAGAGTGACTCACCGTCCTTGACACGATGAGGGCTTGGATCTTCTTTCTGCTCTG
CCTGGCCGGGCGCGCCTTGGCCGATATTCAGATGACTCAGAGCCCCAGCAGCCTGTC
TGCTAGCGTTGGGGATAGAGTCACTATAACATGTCGGGCTTCCCAGGATGTGAATAC
TGCTGTCGCTTGGTATCAACAGAAGCCCGGCAAGGCACCAAAACTGCTGATATATA
GTGCCTCTTTCCTTTACTCCGGGGTTCCCAGTCGATTCTCTGGAAGCCGCAGCGGCA
CTGATTTCACACTTACTATAAGTAGTCTGCAACCTGAGGACTTTGCTACATACTACTG
CCAGCAGCACTATACAACACCCCCAACTTTCGGGCAAGGCACTAAGGTAGAAATTA

AAAGGACCGTTGCTGCTCCATCCGTCTTTATTTTTCCACCATCTGATGAACAGTTGAA
GAGCGGAACAGCAAGCGTCGTTTGTCTCCTGAACAATTTTTACCCACGAGAGGCAA
AAGTTCAATGGAAGGTAGACAATGCTCTTCAGAGCGGCAATTCCCAGGAGAGCGTA
ACCGAGCAGGATAGCAAAGACTCTACATACTCTTTGAGTTCAACCCTTACCCTGAGC
AAGGCTGATTACGAAAAACACAAGGTGTACGCTTGCGAGGTAACCCATCAGGGATT
GTCATCCCCAGTCACAAAATCATTCAATAGGGGCGAGTGCTGACGGGTGGCATCCCT
GTGACCCCTCCCCAGTGCCTCTCCTGGCCCTGGAAGTTGCCACTCCAGTGCCCACCA
GCCTTGTCCTAATAAAATTAAGTTGCATCAAGCT

Supplemental Figure 2. *Alignment of trastuzumab peptides identified in serum of mice injected with trastuzumab mRNA-LNPs with full trastuzumab amino acid sequence.*

```
Trastuzumab Heavy Chain
            10        20        30        40        50                60        70        80        90       100       110
QUERY   EVQLVESGGGLVQPGGSLRLSCAASGFNIKDTYIHWVRQAPGKGLEWVAR---------YADSVKGRFTISADTSKNTAYLQMNSLRAEDTAVYYCSRWGGDGFYAMDYWGQGTLVTVSS
        ::::::::::::::::::::::::::::::::::::::::::::::::::         ::::::::::::::::::::::::::::::::::::::::::::::::::::::::::::::
T-HC    EVQLVESGGGLVQPGGSLRLSCAASGFNIKDTYIHWVRQAPGKGLEWVARIYPTNGYTRYADSVKGRFTISADTSKNTAYLQMNSLRAEDTAVYYCSRWGGDGFYAMDYWGQGTLVTVSS
             10        20        30        40        50        60        70        80        90       100       110       120

           120       130       140                                                                   150       160
QUERY   ASTKGPSVFPLAPSSKSTSGGTAALGCLVK-----------------------------------------------------------VDKKVEPKSCDKTHTCPPCPAPELLGG
        ::::::::::::::::::::::::::::::                                                           ::::::::::::::::::::::::::::
T-HC    ASTKGPSVFPLAPSSKSTSGGTAALGCLVKDYFPEPVTVSWNSGALTSGVHTFPAVLQSSGLYSLSSVVTVPSSSLGTQTYICNVNHKPSNTKVDKKVEPKSCDKTHTCPPCPAPELLGG
            130       140       150       160       170       180       190       200       210       220       230       240

      170       180       190       200       210       220       230       240       250       260       270       280
QUERY   PSVFLFPPKPKDTLMISRTPEVTCVVVDVSHEDPEVKFNWYVDGVEVHNAKTKPREEQYNSTYRVVSVLTVLHQDWLNGKEYK--VSNKALPAPIEK------GQPREPQVYTLPPSREE
        ::::::::::::::::::::::::::::::::::::::::::::::::::::::::::::::::::::::::::::::::::::  ::::::::::::      ::::::::::::::::::
T-HC    PSVFLFPPKPKDTLMISRTPEVTCVVVDVSHEDPEVKFNWYVDGVEVHNAKTKPREEQYNSTYRVVSVLTVLHQDWLNGKEYKCKVSNKALPAPIEKTISKAKGQPREPQVYTLPPSREE
            250       260       270       280       290       300       310       320       330       340       350       360

            290       300       310       320       330       340       350       360
QUERY   MTKNQVSLTCLVKGFYPSDIAVEWESNGQPENNYKTTPPVLDSDGSFFLYSKLTVDKSRWQQGNVFSCSVMHEALHNHYTQK
        ::::::::::::::::::::::::::::::::::::::::::::::::::::::::::::::::::::::::::::::::::::
T-HC    MTKNQVSLTCLVKGFYPSDIAVEWESNGQPENNYKTTPPVLDSDGSFFLYSKLTVDKSRWQQGNVFSCSVMHEALHNHYTQKSLSLSPGK
            370       380       390       400       410       420       430       440       450


Trastuzumab Light Chain
             10              20        30        40        50              60        70        80        90              100
QUERY   DIQMTQSPSSLSASVGDR------ASQDVNTAVAWYQQKPGKAPKLLIYSASFLYSGVPSR-----SGTDFTLTISSLQPEDFATYYCQQHYTTPPTFGQGTK----RTVAAPSVFIFPP
        ::::::::::::::::::      ::::::::::::::::::::::::::::::::::     ::::::::::::::::::::::::::::::::::    :::::::::::::
T-LC    DIQMTQSPSSLSASVGDRVTITCRASQDVNTAVAWYQQKPGKAPKLLIYSASFLYSGVPSRFSGSRSGTDFTLTISSLQPEDFATYYCQQHYTTPPTFGQGTKVEIKRTVAAPSVFIFPP
             10        20        30        40        50        60        70        80        90       100       110       120

          110       120           130       140       150       160       170       180
QUERY   SDEQLKSGTASVVCLLNNFYPR---VQWKVDNALQSGNSQESVTEQDSKDSTYSLSSTLTLSKADYEKHKVYACEVTHQGLSSPVTK
        ::::::::::::::::::::::   ::::::::::::::::::::::::::::::::::::::::::::::::::::::::::::::
T-LC    SDEQLKSGTASVVCLLNNFYPREAKVQWKVDNALQSGNSQESVTEQDSKDSTYSLSSTLTLSKADYEKHKVYACEVTHQGLSSPVTKSFNRGEC
             130       140       150       160       170       180       190       200       210
```

Supplemental Figure 3. *HER2 expression in MDA-MB-231-HER2 cells was measured using RT-qPCR and compared to control MDA-MB-231 cells. Mean±SD, relative to HER2-expression in MDA-MB-231 cells.*

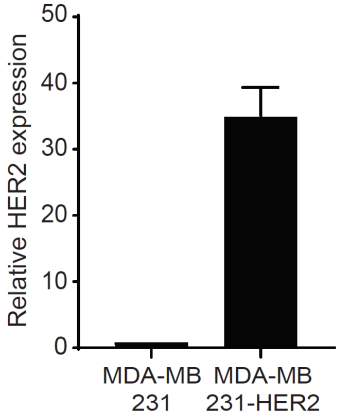

Supplemental Figure 4. *RNA expression in tumor-bearing mice after LNP administration. IVIS imaging of the whole-body (arrowheads point on tumor location) (**A**) and selected organs (**B**) from athymic nude mice 6h after i.v. injection with Firefly liciferase (Fluc) mRNA formulated into LNPs. Bioluminescence scale is radiance (p/sec/cm2/sr).* ***C.*** *Quantification of bioluminescence in selected tissues.*

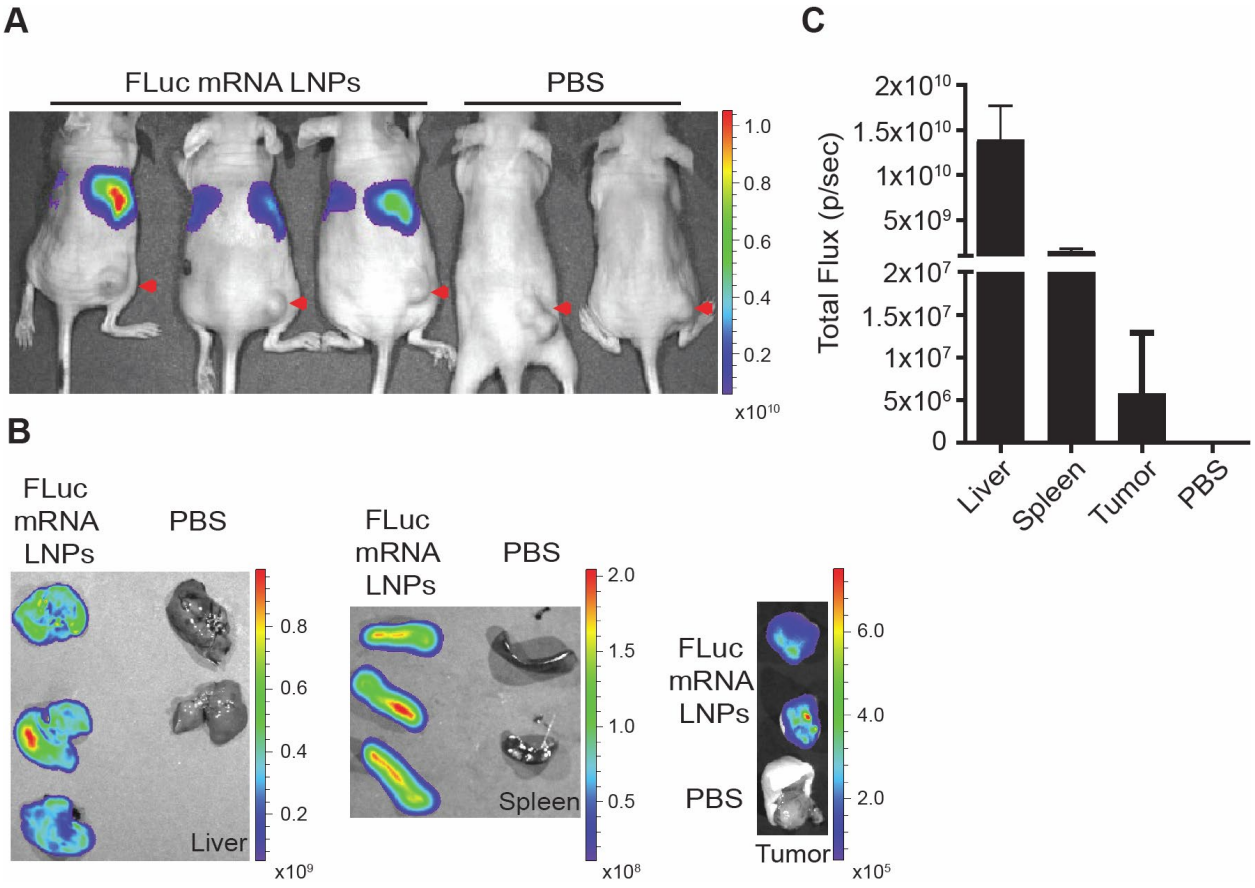

Supplemental Figure 5. Effects of treatment with trastuzumab mRNA LNPs on different organs. *Haematoxylin and eosin staining of livers and spleens from mice with HER-negative (MDA-MB-231) and HER2-positive (MDA-MB-231-HER2) tumors treated with the trastuzumab mRNA or PBS (control). Scale bar, 100 um.*

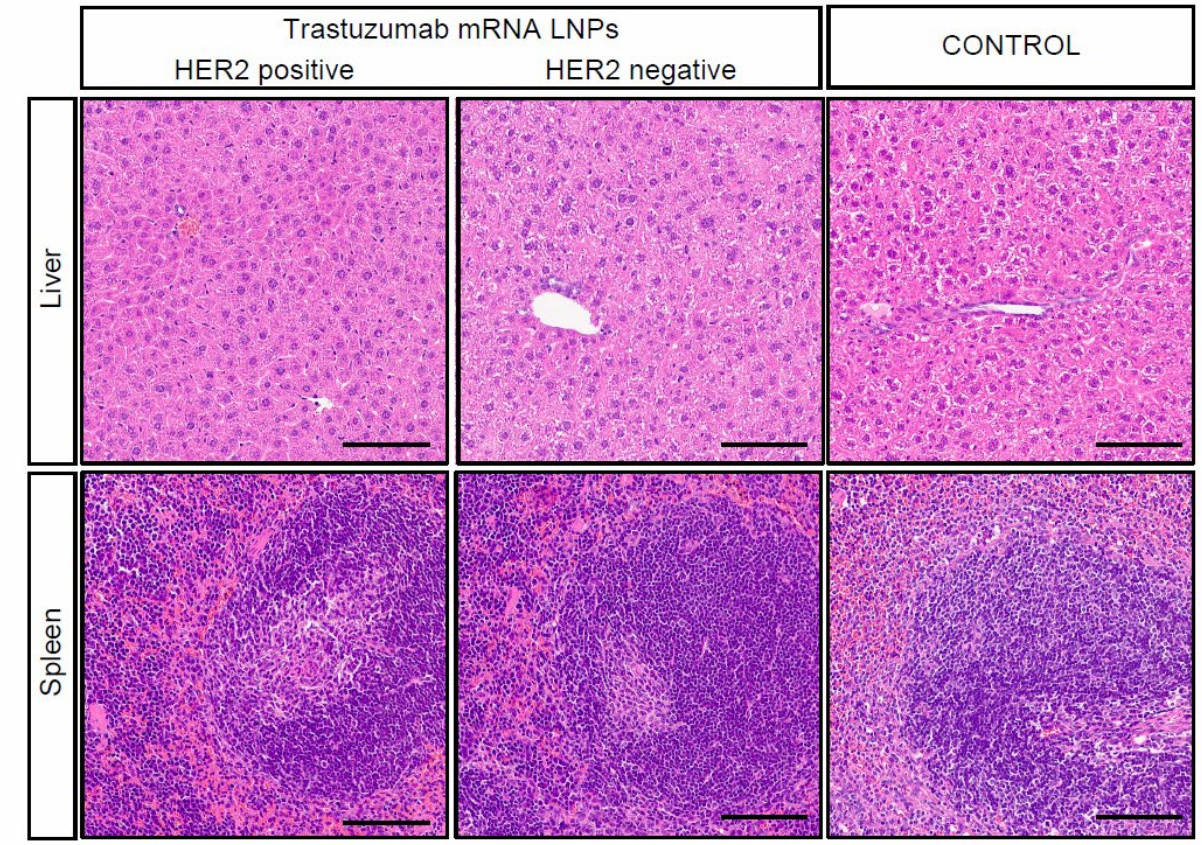

Supplemental Figure 6. *Growth (median±IQR) of HER2-negative (MDA-MB-231) and HER2-positive (MDA-MB-231-HER2) tumors in mice treated with four weekly injections of (**A**) 2 mg/kg trastuzumab mRNA (n=5) or saline (n=6); (**B**) 2 mg/kg trastuzumab mRNA (n=5), 8 mg/kg Herceptin (n=4) or saline (n=6). Two-way repeated measures ANOVA with Sidak multiple comparisons tests, ** p-value ≤ 0.01, **** p-value ≤ 0.0001 for HER2-positive tumors treated with mRNA compared to saline.*

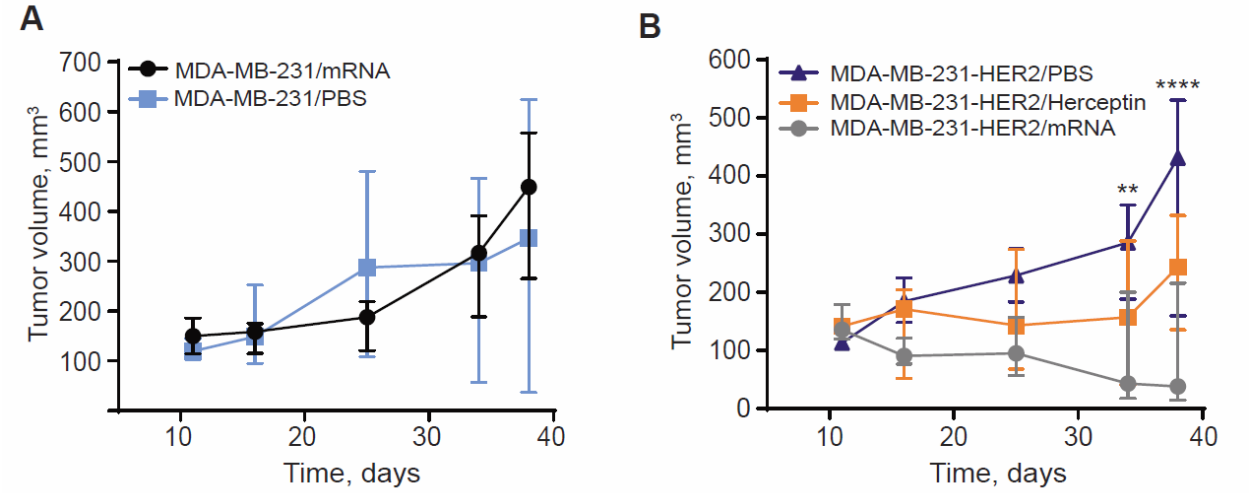

Supplemental Table 1. *Signal peptide sequences used in the study.*

Protein name	Signal peptide sequence
Gaussian luciferase	ATGGGTGTAAAGGTGCTCTTCGCCCTGATATGTATAGCCGTG GCCGAGGCT
Human immunoglobulin light chain kappa	ATGAGGGCTTGGATCTTCTTTCTGCTCTGCCTGGCCGGGCGC GCCTTGGCC
Human immunoglobulin G1 heavy chain	ATGGACTGGACCTGGAGGTTCCTCTTTGTGGTGGCAGCAGCT ACAGGTGTCCAGTCC

Supplemental Table 3. Effects of treatment with trastuzumab mRNA LNPs on blood cell count parameters in athymic nude mice with MDA-MB-231 or MDA-MB-231-HER2 xenografts. *Female athymic nude mice inoculated with MDA-MB-231 or MDA-MB-231-HER2 cells received four weekly i.v. injections of 2 mg/kg trastuzumab mRNA formulated into cKK-E12 nanoparticles or PBS. The serum was collected one week after the final injection. One-way ANOVA followed by Dunnett's post hoc test, * p-value ≤ 0.05, ** p-value ≤ 0.01, *** p-value ≤ 0.001, **** p-value ≤ 0.001 compared to healthy mice.*

Parameter	Units	Healthy mice	Untreated tumor-bearing mice	MDA-MB-231	MDA-MB-231-HER2
		Mean±SD, n=3	Mean±SD, n=3	Mean±SD, n=3	Mean±SD, n=3
Leukocytes:					
WBC	K/ul	10.1 ± 1.6	5.1 ± 1.6	12.4 ± 9.4	5.6 ± 0.2
NE	K/ul	2.6 ± 0.7	1.7 ± 0.8	7.8 ± 7.5	2.7 ± 1
LY	K/ul	7 ± 0.7	3.0 ± 0.6**	3.9 ± 1.6*	2.7 ± 0.8**
MO	K/ul	0.3 ± 0.1	0.2 ± 0.1	0.3 ± 0.2	0.2 ± 0.1
EO	K/ul	0.1 ± 0.1	0.2 ± 0.2	0.2 ± 0.2	0.1 ± 0.0
BA	K/ul	0 ± 0.1	0.1 ± 0.1	0 ± 0	0.1 ± 0.1
Erythrocytes:					
RBC	M/ul	8.1 ± 0.3	6.8 ± 0.1***	8.5 ± 0.2	8 ± 0.2
Hb	g/dL	14.4 ± 0.8	11.3 ± 0.1****	13.3 ± 0.1*	12.8 ± 0.3**
HCT	%	47.4 ± 8.8	36.9 ± 5.6	46 ± 6	38.7 ± 0.5
MCV	fL	58.1 ± 8.2	54.1 ± 7.8	54.3 ± 6.1	48.2 ± 1.7
MCH	pg	17.7 ± 0.9	16.6 ± 0.1	15.7 ± 0.4**	16 ± 0.6*
MCHC	g/dL	30.9 ± 4.9	31 ± 4.1	29.3 ± 3.4	33.2 ± 0.6
RDW	%	15.6 ± 0.2	17.5 ± 0.7**	18.3 ± 0.1***	18.3 ± 0.5***
Thrombocytes:					
PLT	K/ul	688 ± 124	347 ± 270.5	866 ± 128	936 ± 203.5
MPV	fL	4.7 ± 0.1	5.5 ± 0.8	5.3 ± 0.3	5.3 ± 0.1

Supplemental Table 4. Effects of treatment with trastuzumab mRNA LNPs on parameters of serum chemistry in athymic nude mice. *Female athymic nude mice with MDA-MB-231 or MDA-MB-231-HER2 xenografts received four weekly i.v. injections of 2 mg/kg trastuzumab mRNA formulated into cKK-E12 nanoparticles or PBS. The serum was collected one week after the final injection. One-way ANOVA followed by Dunnett's post hoc test, * p-value ≤ 0.05 compared to healthy mice.*

Parameter	Units	Untreated tumor-bearing mice	MDA-MB-231	MDA-MB-231-HER2
		Mean±SD, n=4	Mean±SD, n=3	Mean±SD, n=3
Alk Phos	IU/L	27 ± 16.7	51 ± 15.6	45 ± 3.5
ALT	IU/L	102.3 ± 68.1	128 ± 46.1	71.7 ± 7.6
AST	IU/L	25 ± 4.7	28 ± 5.6	21.7 ± 4
CK	IU/L	499 ± 637	197.5 ± 2.1	118 ± 17.2
GGT	IU/L	0 ± 0	0 ± 0	0 ± 0
Albumin	g/dL	2.5 ± 0.1	2.4 ± 0.3	2.4 ± 0.2
Total Bilirubin	mg/dL	0.1 ± 0.1	0.2 ± 0.1	0 ± 0
Total Protein	g/dL	4.6 ± 0.3	4.2 ± 0.4	4.6 ± 0.3
Globulin	g/dL	2.1 ± 0.2	1.8 ± 0.2	2.2 ± 0.4
Bilirubin- Conjugated	mg/dL	0 ± 0	0 ± 0	0 ± 0
BUN	mg/dL	23.8 ± 4.4	24.7 ± 4.7	18.7 ± 3.8
Creatinine	mg/dL	0.2 ± 0.1	0.1 ± 0.1	0.1 ± 0
Cholesterol	mg/dL	81.3 ± 16.4	102 ± 4.4	87.7 ± 12.9
Glucose	mg/dL	219.5 ± 44.9	246 ± 66	251 ± 16.2
Calcium	mg/dL	7 ± 4.3	8.9 ± 0.9	8.9 ± 0.7
Phosphorus	mg/dL	7.8 ± 1.8	9 ± 1.9	5.9 ± 0.4
Bicarbonate	mEq/L	11 ± 0.8	13 ± 1.7	14.3 ± 1.2*
Chloride	mEq/L	110.3 ± 3.1	112 ± 9.1	111.3 ± 5.8
Potassium	mEq/L	5.9 ± 3.5	5.4 ± 0.9	4.3 ± 0.5
ALB/GLOB ratio	ratio	1.2 ± 0.1	1.4 ± 0.1	1.1 ± 0.3
Sodium	mEq/L	148 ± 2.6	148 ± 13.1	147 ± 8.6
BUN/Creatinine ratio	ratio	107.5 ± 79.8	177 ± 157	187 ± 37.9
Bilirubin-Unconjugated	mEq/L	0.1 ± 0.1	0.2 ± 0.1	0.1 ± 0
NA/K	ratio	30.3 ± 12	28 ± 6.6	34.3 ± 6
Anion Gap	mEq/L	32.8 ± 3.6	28.7 ± 3.5	25.3 ± 2.1*

Supplemental Table 5. *Physicochemical properties of RNA nanoparticles. Particle size and the Polydispersity index were analyzed by dynamic light scattering using Zetasizer Nano (Malvern). Encapsulation efficacy was determined with the Quant-iT Ribo-Green assay (Invitrogen). HC – heavy chain, LC – light chain. Data are presented as Mean ±SD, n=3.*

Trastuzumab HC mRNA to LC mRNA ratio	Polydispersity	Size Intensity mean (nm)	Encapsulation efficacy (%)
1:1	0.14 ± 0.02	103 ± 3	71 ± 6
1:2	0.13 ± 0.01	104 ± 5	76 ± 3
1:4	0.15 ± 0.02	101 ± 3	72 ± 4

Supplemental Methods

Generation of MDA-MB-231-HER2 cell line. MDA-MB-231 cells were retrovirally transduced with human HER2 (MSCV-human Erbb2-IRES-GFP, Addgene #91888). Green fluorescent protein (GFP) positive cells were sorted by FACS, HER2 expression in the selected cells was confirmed by RT-qPCR using HER2-FWD GAAGCCTCACAGAGATCTTG and HER2-REV CCTTACACATCGGAGAACAG primers (from (57)).

Cell-based assays. For transfection with mRNA 500-700 000 cells were seeded per well in 6-well plates. Within 24h the cells were transfected with mRNA using Lipofectamine™ MessengerMAX™ Reagent (Thermo Fisher Scientific) according to the manufacturer's protocol. Breast cancer cell survival was analyzed using CellTiter-Glo® Luminescent Cell Viability Assay according to the manufacturer's protocol. Briefly, 15 000 cells were plated per well in 96 well plate. Next day cells were treated with trastuzumab isolated from mouse blood or with Herceptin (Genentech). Two days after the treatment CellTiter was added to the cells and luminescence was measured by microplate reader Tecan Infinite® 200 PRO.

IVT-mRNA synthesis. IVT-mRNA synthesis was performed as previously described (Kauffman et al, 2015, 2016). Briefly, DNA plasmids containing a T7 promoter upstream of the sequences of trastuzumab heavy or light chain were linearized and transcribed using the HiScribe T7 RNA Synthesis Kit (New England Biolabs (NEB). mRNA was capped with the Vaccinia Capping System (NEB), and polyA tails were added to the RNA using a Poly(A) Polymerase Kit (NEB).). All mRNAs were purified after the transcription and tailing steps using MEGAClear RNA purification kit according to manufacturer protocol (Life Technologies). Final purified mRNAs contained a 5' cap (Cap1), a 5' UTR consisting of a partial sequence of the cytomegalovirus (CMV) immediate early 1 (IE1) gene, a coding region as described below, a 3' UTR consisting of a partial sequence of the human growth hormone (hGH) gene, and a 3' polyA tail estimated to be approximately 120 nucleotides long.

IVT-mRNA formulation into LNPs. LNPs were prepared by mixing ethanol and aqueous phase at a 1:3 volumetric ratio in a microfluidic device, using syringe pumps as previously described (Chen, Love et al., 2012). The ethanol phase was prepared by solubilizing a mixture of ionizable lipidoid cKK-E12, 1,2-dioleoyl-sn-glycero-3-phosphoethanolamine (DOPE, Avanti), cholesterol (Avanti), and 1,2-dimyristoyl-sn-glycero-3-phosphoethanolamine-N-[methoxy-(polyethyleneglycol)-2000] (ammonium salt) (C14-PEG 2000, Avanti) at a molar ratio of 35:16:46.5:2.5 The aqueous phase

was prepared in 10 mM citrate buffer (pH 3) with either trastuzumab mRNA or luciferase mRNA (Firefly luciferase mRNA, TranslateBio). LNPs were dialyzed against PBS in a Slide-A-Lyzer™ G2 Dialysis Cassettes, 20,000 MWCO (Thermo Fisher) for 2h at RT. The concentration of mRNA encapsulated into LNPs nanoparticles was analyzed using Quant-iT RiboGreen assay (Thermo Fisher), according to manufacturer's protocol. The efficacy of mRNA encapsulation into LNPs was calculated by comparing measurements in the absence and presence of 1% (v/v) Triton X-100. Nanoparticle size, polydispersity (PDI), and ζ-potential were analyzed by dynamic light scattering (DLS) using Zetasizer Nano ZS (Malvern Instruments, Worcestershire, UK). LNP hydrodynamic diameters are reported in the volume weighting mode and are an average of three independent measurements (Supplemental Table 5).

Biodistribution analysis. cKK-E12 LNPs containing Firefly Luciferase mRNA (TranslateBio) were injected intravenously into female athymic nude mice via tail vein (2 mg kg-1). 6 h after the injection of the nanoparticles, mice were injected intraperitoneally with 130 μL of D-luciferin (30 mg mL-1 in PBS, Perkin Elmer). After 10 min, mice were sacrificed by CO2 asphyxiation and both tumors and organs (liver and spleen) were isolated and imaged with an IVIS Spectrum In Vivo Imaging System (PerkinElmer). Florescence signals were quantified using Living Image software v4.4 (PerkinElmer).

Histological analysis. Freshly collected tissues were fixed in 4% paraformaldehyde and embedded into paraffin. Four-micrometer-thick sections were subjected to hematoxylin and eosin staining.

ELISA. Tratsuzumab levels were measured using Invitrogen™ IgG1 Human ELISA Kit (cat. #EHIGG1) (Figure 1) or AffinityImmuno Trastuzumab (Herceptin®) Pharmacokinetic ELISA (cat. #EL-1611-201) (Figure 2) according to manufacturers' instructions.

Mass Spectrometry studies were performed by Swanson Biotechnology Center at David. H Koch Institute for Integrative Cancer Research at MIT. *IgG enrichment*: Herceptin was isolated from the samples using the Pierce MS-compatible IP kit protein A/G per manufacturer's instructions. 25 uL of beads were used for 1 ug of Herceptin (determined via ELISA). Beads were washed with lysis buffer, added to the Herceptin containing samples, and incubated at r.t. for 1 h on a rotator. The beads were then washed three times with wash buffer A, three times with wash buffer B, and three times with 100 mM ammonium bicarbonate, pH 8. *Reduction, Alkylation, and Tryptic Digestion*: On-bead reduction, alkylation, and digestion was performed. Proteins were reduced with 10 mM dithiothreitol (Sigma) for 1h at 56ºC and then alkylated with 55 mM iodoacetamide (Sigma) for 1h at 25ºC in the dark. Samples were incubated with PNGaseF for 2 h at 37ºC. Proteins were then digested with modified trypsin (Promega) at an enzyme/substrate ratio of 1:50 in 100 mM ammonium bicarbonate, pH 8 at 25ºC overnight. Trypsin activity was halted by addition of formic acid (99.9%, Sigma) to a final concentration of 5%. Peptides were desalted using C18 SpinTips (Protea, Morgantown, WV) then vacuum centrifuged and stored at −80 °C. *LC-MS/MS*: Peptides were loaded on a precolumn and separated by reverse phase HPLC using an EASY- nLC1000 (Thermo) over a 75 minute gradient before nanoelectrospray using a QExactive HF-X mass spectrometer (Thermo). The mass spectrometer was operated in a data-dependent mode. The parameters for the full scan MS were: resolution of 70,000 across 350-2000 m/z, AGC 3e6, and maximum IT 50 ms. The full MS scan was followed by MS/MS for the top 15 precursor ions in each cycle with a NCE of 28 and dynamic exclusion of 30 s. Raw mass spectral data files (.raw) were searched using Proteome Discoverer 2.2 (Thermo) and Mascot version 2.4.1 (Matrix Science). Mascot search parameters were: 10 ppm mass tolerance for precursor ions; 15 mmu for fragment ion mass tolerance; 2 missed cleavages of trypsin; fixed modification was carbamidomethylation of cysteine; variable modifications were methionine oxidation, asparagine

deamidation. Only peptides with a Mascot score greater than or equal to 25 and an isolation interference less than or equal to 30 were included in the data analysis.

Gene expression analysis. RNA was isolated using Omega Bio-tek The E.Z.N.A.® Total RNA Kit I isolation kit according to manufacturers' instructions. Reverse transcription reaction was performed using Applied Biosystems™ High-Capacity RNA-to-cDNA™ Kit and 1 ug of RNA. Levels of mRNAs were assessed by qPCR using Roche LightCycler 480. β-actin mRNA was used as housekeeping controls. The mRNA levels were normalized to the level of β-actin gene and to an average value of control group.

The analysis of pharmacokinetic properties of trastuzumab. Pharmacokinetic parameters of Trastuzumab were calculated using PKSolver 2.0 software (58). Non-compartmental analysis was performed on ELISA datasets (Affinity Immuno, Pharmacokinetic Trastuzumab ELISA) measuring trastuzumab concentration in mouse serum samples collected over the course of 30 days.